JACS
JOURNAL OF THE AMERICAN CHEMICAL SOCIETY

pubs.acs.org/JACS

Article

Hypervalent Iodine(III) Compounds as Biaxial Halogen Bond Donors

Flemming Heinen, Elric Engelage, Christopher J. Cramer, and Stefan M. Huber*

Cite This: J. Am. Chem. Soc. 2020, 142, 8633−8640

Read Online

ACCESS | Metrics & More | Article Recommendations | Supporting Information

ABSTRACT: "Hypervalent" iodine(III) derivatives have been established as powerful reagents in organic transformations, but so far only a handful of studies have addressed their potential use as halogen-bonding noncovalent Lewis acids. In contrast to "classical" halogen-bond donors based on iodine(I) compounds, iodine(III) salts feature two directional electrophilic axes perpendicular to each other. Herein we present the first systematic investigation on biaxial binding to such Lewis acids in solution. To this end, hindered and unhindered iodolium species were titrated with various substrates, including diesters and diamides, via ^{1}H NMR spectroscopy and isothermal titration calorimetry. Clear evidence for biaxial binding was obtained in two model systems, and the association strengths increased by 2 orders of magnitude. These findings were corroborated by density functional theory calculations (which reproduced the trend well but underestimated the absolute binding constants) and a cocrystal featuring biaxial coordination of a diamide to the unhindered iodolium compound.

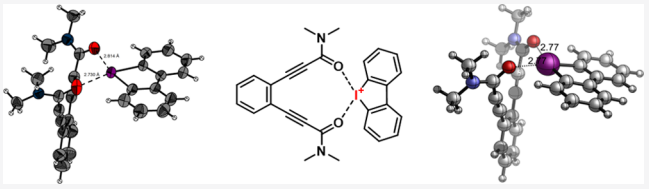

INTRODUCTION

The chemistry of hypervalent iodine (HVI) compounds is known for its versatility in organic reactions.[1] Iodine(III) species, for instance, are established in a wide range of organic transformations, such as the oxidation of functional groups[2] or as transition-metal catalyzed[3] or direct[3a,4] arylating agents. In the latter case, diaryl iodonium species are often applied. These typically feature a T-shaped structure with the two aryl substituents bound to iodine in a roughly 90° angle and the anion bound via an additional "secondary" bonding.[1a] This interaction between the iodonium cation and its anion vividly illustrates the electrophilic nature of the iodine center, and the coordination can be seen as a special case of halogen bonding (the noncovalent interaction between electrophilic halogen substituents and Lewis bases).[5] Halogen bonding is based on contributions from electrostatics,[6] charge transfer,[7] and dispersion, and one of its key features is its high linearity, that is, interaction angles of ∼180°. Iodine(I)-based Lewis acids have by now been used in various applications, for example, in crystal engineering,[8] molecular recognition,[5,9] and catalysis.[10]

Even though the Lewis acidity of iodine(III) species has implicitly been exploited in countless instances in synthesis, the organoiodine compounds act as reagents in all these cases. The explicit use of iodine(III)-based Lewis acidity, in contrast, has only been studied and applied in very few examples so far: Liu et al. applied diaryl iodonium salts as Lewis acids in a threefold Mannich reaction,[11] whereas Legault et al. quantified the Lewis acidity of iodine(III) compounds and compared their strength with other classical Lewis acids.[12] Recently, our group reported the use of cyclic iodolium compounds in two benchmark reactions, namely, the solvolysis of benzhydryl chloride with acetonitrile and a classical Diels−Alder reaction.[13]

In all these cases, however, only one electrophilic axis on the iodine atom has been used to bind to Lewis bases despite the fact that iodine(III)derivatives—in contrast to iodine(I) species—feature *two* such electrophilic axes in elongation of both R−I bonds (Figure 1).

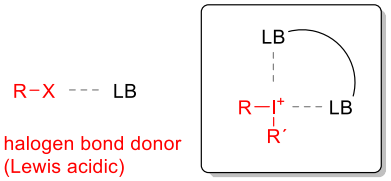

Figure 1. Comparison of binding modes of binding events to Lewis bases between an iodine(I) XB donor (left) and a biaxial iodine(III) XB donor (right).

This has been confirmed by several theoretical studies[14] and also by various solid-state structures, as it is well-known that diaryliodonium halides form dimers in which two halides are bound to each iodine(III) center.[15] Somewhat surprisingly, to the best of our knowledge, there is currently only one application that is based on the simultaneous use of both electrophilic axes: Ochiai and co-workers used crown ethers to complex to iodine(III) species like ethynyl(phenyl)-λ^3-iodanes in order to increase their thermal stability. Crystal structures provided

Received: December 10, 2019
Published: April 14, 2020

https://dx.doi.org/10.1021/jacs.9b13309
J. Am. Chem. Soc. 2020, 142, 8633−8640

evidence of two-point binding between two oxygen atoms of the crown ether and both axes of the iodine center, and titrations in solution confirmed stronger binding compared to open-chain variants like diglyme.[16] However, because of the presence of three or more oxygen atoms on the Lewis bases, there is no ideal match between halogen bond donor and acceptor, and in addition also the reference compounds (like diglyme) likely bind in a two-point fashion. Thus, there is currently no systematic comparison of biaxial versus monoaxial binding and no investigation of their relative strength. Herein, we present such a study, featuring the biaxial binding of a neutral bidentate Lewis base to an iodolium salt, supported by density functional theory (DFT) calculations, ^{1}H NMR titrations, isothermal titration calorimetry (ITC) titrations, and X-ray diffraction (XRD) analyses.

RESULTS AND DISCUSSION

Orientating Computational Screening. Iodolium cations were chosen as halogen-bond donors, since they feature a very rigid geometry, which also allows to block one or both electrophilic axes by substituents in α-position to the iodine center.[13] In order to identify suitable bidentate Lewis bases that are capable of binding to both electrophilic axes of these donors simultaneously, we performed DFT calculations (M06-2X[17]/def2-TZVP(D)[18]/SMD18;[19] for further details see below). Initially investigated substrates were based on malonic acid derivatives, which bear two carbonyl groups in close proximity (complex **1**, Figure 2). The calculations revealed, however, that

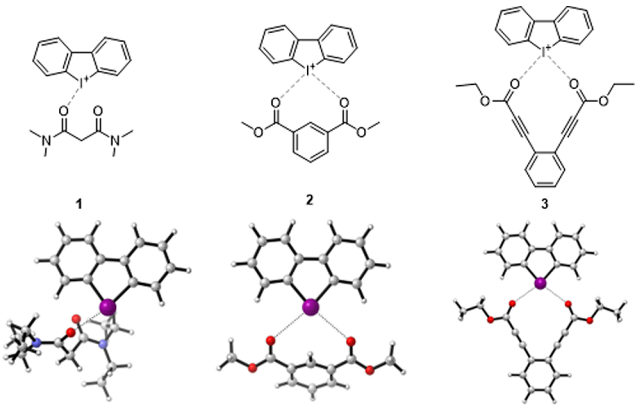

Figure 2. Schematic representation of complexes involving biaxial halogen bonding to iodolium (top) and complexes obtained via DFT calculations in chloroform (M06-2X[17]/def2-TZVP(D)[18]/SMD18,[19] bottom). Graphics generated with CYLview.[20]

the distance between the two oxygens is too short, and thus only a single halogen bonding interaction is found. Instead, biaxial binding was found in complexes with isophthalic acid (**2**) or diethyl-3,3′-(1,2-phenylene)dipropiolate (**3**) in chloroform, and symmetrical adducts with two identical halogen bonds were obtained (Figure 2).

^{1}H NMR and ITC Titration Experiments. To confirm the formation of these complexes in solution, binding constants of various ketones, esters, and amides to iodolium/BAr^F_4 **4a** (Figure 4) in $CDCl_3$ were determined by ^{1}H NMR titrations. Figure 3 (top) illustrates the binding event between iodolium/BAr^F_4 **4a** and diester **5** with a typical fitting curve of the ^{1}H NMR titration (middle) and the relevant ^{1}H NMR data set indicating the shifting signals of the α-protons (bottom). If compounds like

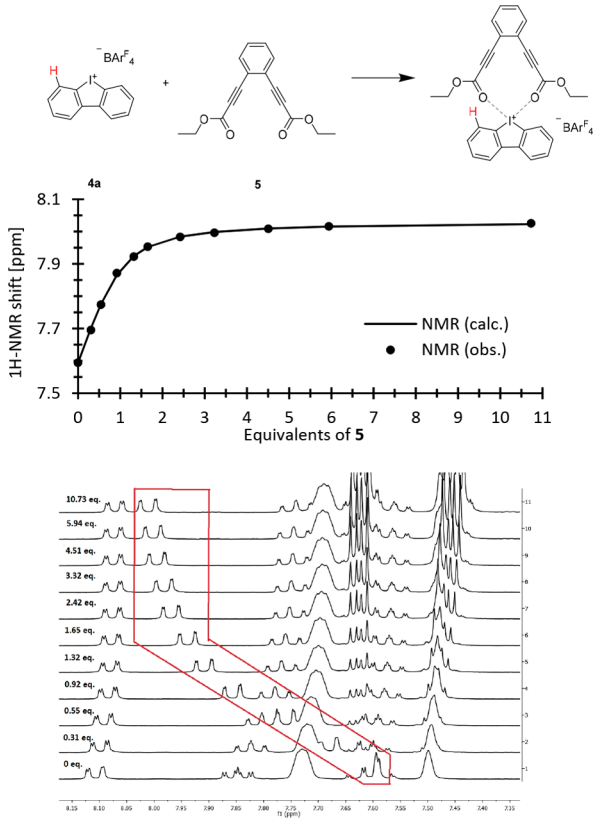

Figure 3. Exemplified binding event between iodolium/BAr^F_4 **4a** and diester **5** (top) with their typical fit curve (middle) and the corresponding raw ^{1}H NMR data (bottom) for the determination of their binding constant.

diester **5** would bind in a biaxial manner, stronger complexation should occur compared to electronically similar structures, which cannot coordinate in such a fashion due to geometric constraints. The experimental data are summarized in Figure 4.

Indeed, a comparison of diesters **5** and **7**, which only differ in their substitution pattern but are otherwise electronically identical, clearly demonstrates biaxial binding of the former to the iodolium. DFT calculations confirm that only one carbonyl of **7** is bound to the Lewis acid (see Supporting Information). This leads to very marked differences in the measured binding constants: while *ortho*-diester **5** showed an association strength of $K = 1.0 \times 10^3$ M^{-1}, *para*-diester **7** featured a significantly lower value of $K = 1.7 \times 10^1$ M^{-1}. Thus, biaxial adduct formation increases the binding strength by at least 2 orders of magnitude.

To underline the significant relative binding strength of diester **5**, an array of further esters and ketones, including α-alkyne, α-alkene, and cyclic esters/ketones, was also tested. In general, esters **9**, **11**, and **12** show very similar binding constants of $\sim K = 1.0 \times 10^1$ M^{-1}, which is in good agreement with the value found for the monoaxially binding diester **7**. Interestingly, these data also indicate that diester **9**, which was found to bind in a biaxial fashion in DFT calculations (complex **2**, Figure 2), acts as a monodentate Lewis base.

In comparison to the open-chain systems, cyclic ester **16** gave a higher binding constant of $K = 1.0 \times 10^2$ M^{-1}, which was also superior to the one of structurally related cyclohexanone (**15**). Ketones **10** and **13**, in contrast, were found to bind stronger ($K = 2.6–4.8 \times 10^1$ M^{-1}) than the corresponding open-chain esters.

Motivated by these findings, the experiments were expanded toward amides. Their increased Lewis basicity should lead to

https://dx.doi.org/10.1021/jacs.9b13309
J. Am. Chem. Soc. 2020, 142, 8633−8640

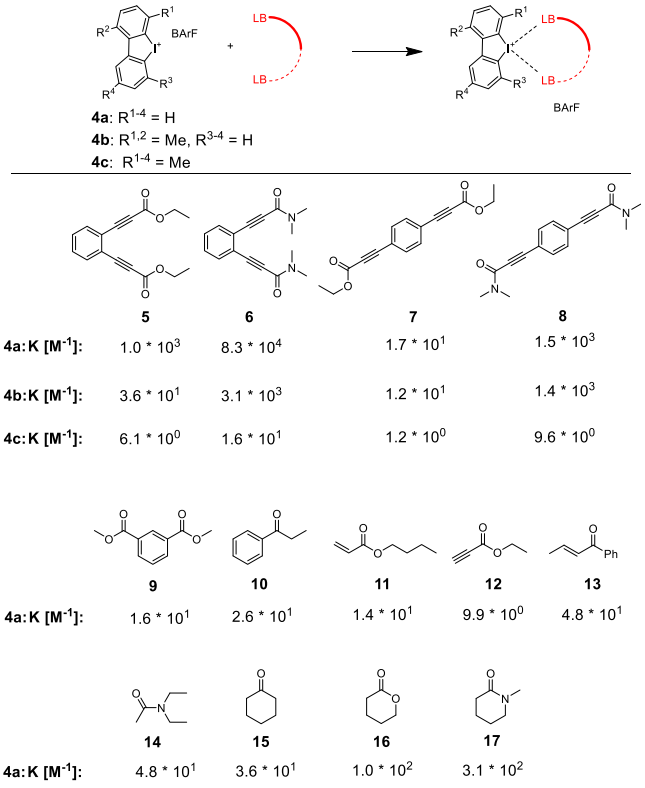

Figure 4. Binding constants of various Lewis bases to XB-Donors **4a**–**4c**. Binding constants were measured via ^{1}H NMR titrations in $CDCl_3$ at 300 K or via ITC experiments at 303 K. For a related figure that is based on free energies, see the Supporting Information (Figure S38).

higher binding constants for isostructural motifs. Similar to the esters **5** and **7**, we expected a significant difference in binding constants for the corresponding *ortho*- and *para*-substituted diamides **6** and **8**. Because of stronger binding, the association constant of diamide **6** could be determined via ITC experiments, and a representative measurement is shown in Figure 5.

While the diamide **6** gave a value of $K = 8.3 \times 10^4$ M^{-1}, here again the electronically similar compound **8** resulted in a significantly lower complexation constant of $K = 1.5 \times 10^3$ M^{-1}. As with the pair of diesters **5** and **7**, the difference in binding is ~2 orders of magnitude. It is noteworthy that, although a high ΔG value of −6.7 kcal/mol was detected for the binding of **6** to iodolium **4a**, according to ITC only −1.1 kcal/mol results from enthalpy, and thus the complexation is clearly entropy-driven.

Screening of amides **14** and **17** as substrates indicates that amides indeed bind more strongly to iodolium **4a** than esters (values of $K = 4.8 \times 10^1$ and 3.1×10^2 M^{-1}) and that, in this case, diamide **8** seems to be more Lewis basic than the monodentate analogues.

In a recent publication,[13] we showed that the binding sites of iodolium compound **4a** can be selectively blocked by introduction of methyl substituents *ortho* to the iodine. Herein we want to use these blocked systems **4b** and **4c** to further confirm the biaxial binding of substrates **5** and **6** to the unblocked parent compound **4a** in solution. By blocking one electrophilic axis in derivative **4b** (Figure 4), only monoaxial binding should be possible for these substrates, and thus their association energies should be markedly reduced. In contrast, monodentate substrates **7** and **8** should still be able to bind to one electrophilic axis, and thus no significant change in binding is expected. Indeed, on the one hand, a significant drop in

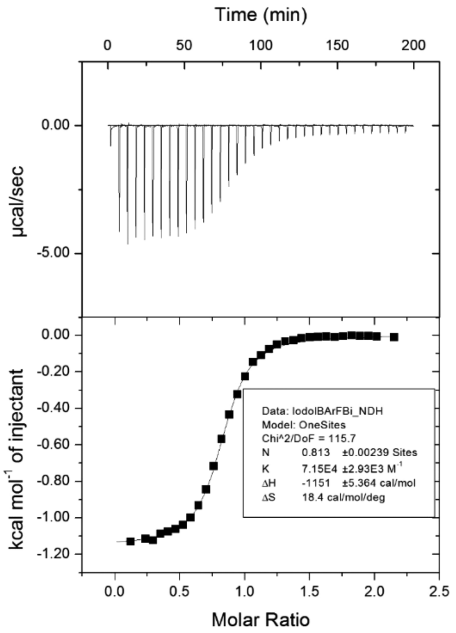

Figure 5. ITC measurement of the complexation of iodolium/BAr^F_4 **4a** with diamide **6** in $CHCl_3$ at 304 K.

binding strength was measured for the complexation of **5** and **6** to **4b** with comparable values of $K = 3.5 \times 10^1$ M^{-1} and $K = 3.1 \times 10^3$ M^{-1}, respectively. On the other hand, the values for substrates **7** and **8** are similar to the ones with the unhindered system **4a**, as expected. Finally, when both electrophilic axes are blocked in derivative **4c**, weak and somewhat comparable binding constants are obtained for all substrates ($K = 1.2$–9.6×10^0 M^{-1}), which are possibly due to π–π interactions.

Theoretical Modeling of Binding Energies. As already indicated above, our experimental studies were accompanied by DFT calculations (using the Gaussian16 software suite, Rev. B.01),[22] which were first performed as described in our previous report on the SMD18 solvation model:[19] the M06-2X[17] density functional was applied in combination with the def2-TZVP[18] basis set, with additional diffuse functions (def2-TZVPD[18]) and the corresponding pseudopotential on iodine.[23] All geometries were fully optimized with the SMD18 intrinsic solvation model[24] using parameters for chloroform on an ultrafine grid. The identity of minima was confirmed by the absence of imaginary frequencies (except for three cases, for which persistent low-lying imaginary frequencies less than −50 cm^{-1} were transformed to positive ones; see the Supporting Information). All frequencies were scaled by 0.9753, as recently determined for the M06-2X def2-TZVP(D) combination.[23] Gibbs free energies were computed at 300 K and were corrected to account for the 1 M standard state in solution.

Overall, these calculations served several purposes: first and foremost, they helped to identify suitable interaction pairs for biaxial binding, as already discussed above (see Figure 2). Second, they test the feasibility of predicting useful binding constants for such kinds of complexes in silico. In our previous study,[19] very good agreement with experimental data was achieved with the above-mentioned protocol and additional corrections for low-frequency entropy issues, as published by Grimme.[25] Such calculations were performed for the complexes of **4a** with all substrates **5**–**17** and for the complexes of **4b** and **4c** with substrates **5**–**8** (the most relevant substrates for biaxial coordination). For all Lewis acid/base pairs, alternative modes

https://dx.doi.org/10.1021/jacs.9b13309
J. Am. Chem. Soc. 2020, 142, 8633–8640

Table 1. Comparison of Experimental and Calculated Gibbs Free Energies ΔG of Adduct Formation

complex		experimental	calculated with SMD				calculated with PCM			
		ΔG	ΔG	AE[a]	ΔG_{Gr}[b]	AE_{Gr}[d]	ΔG	AE	ΔG_{Gr}	AE_{Gr}
4a	**5**	−4.1	−3.7	0.4	−2.0	2.1	−3.3	0.8	−2.0[c]	2.1
	6	−6.3	−9.1	2.8	−7.6	1.3	−6.6[c]	0.3	−6.7	0.4
	7	−1.7	2.3	4.0	4.4	6.1	1.2[c]	0.5	5.1	6.8
	8	−4.4	−1.3[c]	3.1	0.1[c]	4.5	−2.8[c]	1.6	−0.7[c]	3.7
	9	−1.7	0.0[c]	1.7	2.8	4.5	0.4[c]	1.3	3.1[c]	4.8
	10	−2.0	0.7	2.7	2.9	4.9	0.3	2.3	2.6	4.6
	11	−1.6	−1.5	0.1	1.1	2.7	0.4	2.0	2.3	3.9
	12	−1.4	0.1	1.5	2.4	3.8	−0.1	1.3	2.4	3.8
	13	−2.1	−1.7	0.4	0.7	2.8	−2.8	0.7	0.5	2.6
	14	−3.2	−2.1	1.1	−0.1	3.1	−2.0	1.2	−0.1	3.1
	15	−2.1	−0.4	1.7	1.9	4.0	0.2	2.3	2.3	4.4
	16	−2.8	−3.3	0.5	−1.1	1.7	−2.1	0.7	−0.1	2.7
	17	−3.4	−3.9	0.5	−2.0	1.4	−3.1	0.3	−1.2	2.2
4b	**5**	−2.1	−1.3	0.8	0.5	2.6	−1.0	1.1	0.9	3.0
	6	−4.8	−3.6	1.2	−3.8	1.0	−1.7	3.1	0.1	4.9
	7	−1.5	2.7	4.2	5.5	7.0	2.5	4.0	5.6	7.1
	8	−4.3	1.0	5.3	3.0	7.3	1.7	6.0	3.5	7.8
4c	**5**	−1.1	0.2	1.3	0.3[c]	1.4	−1.6[c]	0.5	−1.6	0.5
	6	−1.6	−0.8[c]	0.8	−1.0[c]	0.6	−3.0[c]	1.4	−3.6	2.0
	7	−0.1	7.8	7.9	9.7	9.8	3.6	3.7	4.3	4.4
	8	−1.4	2.9	4.3	5.1	6.5	1.4	2.8	4.3	5.7
MAE[e]				**2.2**		**3.8**		**1.8**		**3.8**

[a]Absolute error (calculation vs experiment). [b]ΔG including low-frequency entropy corrections by Grimme. [c]A more stable conformer (e.g., based on π-stacking) was found. [d]Absolute error for corrected ΔG values (calculations vs experiment). [e]Mean absolute errors.

of association next to halogen bonding were also considered, that is, π-stacking-like interactions. In some cases, particularly for the complexes involving the sterically blocked halogen bond donors, the "π-stacking" variants were found to be energetically more favorable. Here, the corresponding association energies of these structures were then used to model the binding event. The Gibbs free energies for all complexes are provided in Table 1 and are compared to the experimental values.

An inspection of the experimental and initially computed values for the complexes of **4a** (Table 1, columns 2 and 5/6) reveals serious shortcomings: while a few complexation energies are predicted with reasonable quantitative accuracy (e.g., within 1.5 kcal/mol for adducts **4a** · **6** and **4a** · **17**), most are off by several kilocalories per mole (up to 6 kcal/mol for **4a** · **7**). In many cases, this leads to the prediction of endergonic association events, in stark contrast to experiment. The situation is similar for the complexes of **4b** and **4c**, but at least the general trend concerning the binding of **4a** versus **4b/c** to the most important substrates **5** and **6** is passably reproduced computationally. Still, the errors of this method seem too large for the theoretical predictions to be of much use.

Since the functional/basis set combination previously yielded results comparable to CCSD(T) CBS data in the gas phase,[23] the intrinsic solvent model was suspected as the most probable cause of these rather large errors. Thus, the calculations were repeated using the polarizable continuum model (PCM) intrinsic solvation model (as implemented in Gaussian16)[26] instead of SMD18 (Table 1, columns 9 and 10). This, however, yielded no particular improvement.

Another potential source of error is the combination of Grimme's correction for erroneous entropy contributions by low frequencies[25] with parametrized solvation models like SMD (solvation model based on density) and PCM. In our previous study on halogen-bonded adducts between cations (iodoimidazolium and iodolium derivatives) and anions (halides and triflate),[19] these corrections significantly improved the quality of the results. It is, however, also conceivable that, for other types of complexes, adding further corrections to Gibbs free energies that were fitted as closely as possible to experiment without specific accounting for variations in rovibrational partition functions may lead to some "double-counting" and thus a worse performance of the theoretical modeling. This was further investigated by analyzing the SMD18 and the PCM data without application of the low-frequency corrections. In both cases, the uncorrected values provided a markedly better fit to experiment (Table 1, columns 3, 4 and 7, 8), although binding energies remain mostly underestimated, which can still lead to predictions of endergonic binding in some cases. The uncorrected PCM data yield slightly lower overall errors than SMD18 for these systems. This is mostly due to the PCM variant showing better agreement with experiment for the complexes of **4a** with substrates **5**−**8** (which are a main focus of the present study) and to a better modeling of some complexes of **4c**. These "outliers" noticeably cloud the performance of SMD18, which otherwise often yields good agreement with experiment. The average errors of PCM (1.8 kcal/mol) and SMD18 (2.2 kcal/mol) seem very good considering the limitations of intrinsic solvation models.

That low-frequency entropy corrections may either improve or worsen the outcome of SMD18 calculations, depending on the system, is concerning and should be subject to further investigations. For halogen bonding, the overall amount of data is still too small to arrive at definite conclusions, but it may be that double counting may occur in complexes involving neutral substrates. Other possible sources of error include computational undersampling of distinct conformations, which might contribute to the equilibrium population of molecular complexes compared to monomers (consistent with under-

https://dx.doi.org/10.1021/jacs.9b13309
J. Am. Chem. Soc. 2020, 142, 8633−8640

estimation of the free energy of complexation in most instances) and the general difficulty of assessing partition function contributions from low-frequency modes associated with relatively weak nonbonded interactions between molecules when those modes are well-described neither as vibrations nor as internal rotations.

Cocrystallization Experiments. To corroborate our findings in solution, cocrystallization experiments were also performed by slow evaporation of water and dioxane. Indeed, a biaxial mode of binding was found in the cocrystal of iodolium **4a**/BAr^{Cl}_4 (which was used instead of $BAr^{F}_4{}^-$ for better crystallization) and diamide **6** (Figure 6, left). Both oxygens of

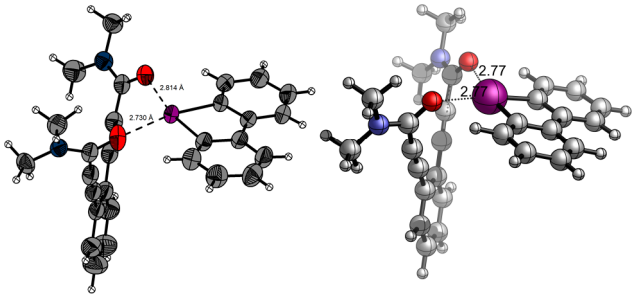

Figure 6. (left) XRD cutout of the complexation between **4a** with BAr^{Cl}_4 as anion and diamide **6**. For clarity the counteranion BAr^{Cl}_4 is omitted. Ellipsoids are set at 50% probability. (right) DFT calculation of the complex in chloroform (M06-2X[17]/def2-TZVPD[18]/SMD18[19]). Visualized with CYL-view.[20]

the diamide are bound to one electrophilic axis of the same iodine center, respectively. The interaction parameters of the complex are typical for halogen bonding, with distances below the sum of the van der Waals radii[21] (2.7 and 2.8 Å vs 3.5 Å) as well as nearly linear C−I···O angles (ca. 177°). The minimum structure calculated with DFT (Figure 6, right) features very similar geometrical data (with almost similar bond distances of 2.77 Å and bond angles of 168°). In both structures, diamide **6** forms an angle of ∼70° to the plane of the iodolium. Thus, while the prediction of absolute energies still seems to be quite challenging for DFT, the structures obtained by such calculations may serve as a very good model for the complex geometries.

Analysis of the Noncovalent Interactions. Finally, the nature of the interaction between the halogen-bond donors and the neutral substrates was analyzed by various quantum-chemical approaches. The key question was whether the main interaction could indeed be described as halogen bonding or whether these associations were simply based on unspecific binding of Lewis basic centers to cations. Obviously, several experimental observations already clearly point toward halogen bonding: the highly linear C−I···O interaction angles in the crystal structure of **4** · **6** (Figure 6) are a typical feature of this interaction, and the fact that complex formation can be strongly suppressed by a blockade of the electrophilic axes associated with halogen bonding further corroborates this. Nevertheless, detailed computational analyses were performed for the complexes exhibiting clear biaxial coordination, that is, the adducts of unsubstituted iodolium compound **4a** with diester **5** and diamide **6**. In both cases, the anion of **4a** was omitted in the calculations.

First, natural bond orbital (NBO) analyses[27] were performed to obtain an orbital-based description of the adduct formation (for further details see Supporting Information). The arguably first theoretical description of halogen bonding by Mulliken[28] was based on the interaction between a lone pair of the Lewis base with the antibonding orbital of the element−halogen bond. This n → σ^* interaction was also identified by NBO second-order perturbation analyses as the key component of intermolecular contact: in the complex **4a** · **5**, the orbital interactions between oxygen lone pairs of **5** and the C−I σ^* orbitals of **4a** were found to be the predominant contribution to the binding, with estimated interaction energies of 2.7 kcal/mol (for sp-hybridized oxygen orbitals on **5**) and 1.4 kcal/mol (for p-hybridized oxygen orbitals on **5**; see Supporting Information). No other intermolecular interaction exceeded 1 kcal/mol. Completely analogous results were obtained for the complex of **4a** with **6**. Here, the corresponding estimated contributions amounted to 5.1 and 2.6 kcal/mol, respectively, and again no other relevant orbital interactions were found. While the energies just mentioned follow the trend in binding strength observed experimentally, their absolute value should probably not be overinterpreted. Still, the NBO analysis clearly confirms halogen bonding as the dominating force for adduct formation.

Further insight was then sought by quantum theory of atoms in molecules (QTAIM)[29] analyses, which were conducted via Multiwfn[30] on wfn files generated by Gaussian. In both complexes, four (3/−1) bond critical points (BCPs) were found between halogen-bond donor and substrate. For adduct **4a** · **5**, these are illustrated, together with the corresponding bond paths, in Figure 7.

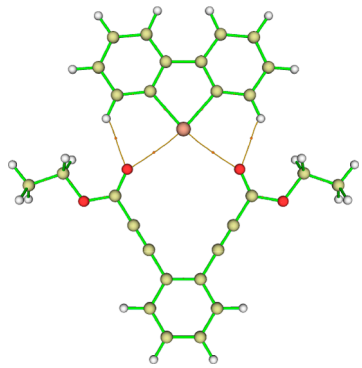

Figure 7. Bond paths and (3/−1) BCPs in the complex of iodolium species **4a** (anion omitted) with diester **5**.

The two outer BCPs correspond to hydrogen bonding between oxygen lone pairs of **5** and the α-protons of **4a**. We note that we had already seen in earlier calculations involving the coordination of a carbonyl group (of a Diels−Alder transition state) to the same iodolium compound **4a** that a strong halogen bond between oxygen and iodine is accompanied by a relatively weak hydrogen bond of the oxygen to the nearest iodolium hydrogen.[13] The two inner BCPs, with density $\rho = -0.14 \times 10^{-1}$ a.u. and Laplacian $\nabla^2 \rho = 0.71 \times 10^{-1}$ a.u., represent halogen bonding. Bond critical points like the ones found here, with relatively small densities ρ and positive Laplacians ($\nabla^2 \rho$), are characteristic for noncovalent intermolecular interactions like hydrogen bonding (and halogen bonding).[29,31] Virtually identical results were obtained for the complex **4a** · **6** (see Supporting Information). The corresponding parameters for the halogen-bonding BCPs are $\rho = -0.20 \times 10^{-1}$ a.u. and $\nabla^2 \rho = 0.84 \times 10^{-1}$ a.u., which are clearly very similar to the ones mentioned above for complex **4a** · **5**.

https://dx.doi.org/10.1021/jacs.9b13309
J. Am. Chem. Soc. 2020, 142, 8633−8640

In addition, the Multiwfn software was also applied to perform noncovalent interaction (NCI) analyses.[32] Once again, analogous results were observed for both biaxial adducts. Scatterplots of reduced density gradient (RDG) versus sign-$(\lambda_2)\rho$ yielded spikes of data points with slightly positive RDG and negative sign$(\lambda_2)\rho$ (see Supporting Information), which indicate attractive intermolecular interactions and are typical for hydrogen bonding and halogen bonding.[32] The corresponding NCI plots clearly provided evidence for attractive noncovalent interactions between the oxygen atoms of **5** and **6** with the iodine center in **4a** (see the bluish surface in Figure 8, which depicts complex **4a** · **6**, and Supporting Information).

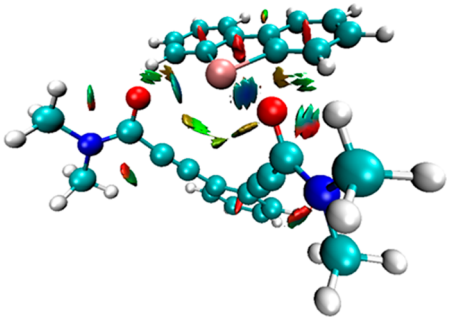

Figure 8. NCI plot for complex **4a** · **6**. Color code: red = repulsion, green = van der Waals attraction/weak interaction (e.g., hydrogen bonding, halogen bonding), blue = strong interaction (hydrogen bonding, halogen bonding).

Thus, NBO, QTAIM, and NCI analyses all unambiguously point toward halogen bonding as the key mode of interaction in complexes **4a** · **5** and **4a** · **6**.

CONCLUSIONS

The first systematic study on the biaxial coordination of iodine(III)-based Lewis acids with suitable bidentate substrates was presented. This model system was investigated by analyzing the binding constants of a series of Lewis bases to three different iodolium compounds via ^{1}H NMR (and in one case ITC) titrations. Biaxial coordination was only achieved in the combination of an unhindered iodolium species with geometrically suitable diesters and diamides. A variation of the bite angle of the latter two substrates, which impedes biaxial binding, led to a reduction in binding strength by 2 orders of magnitude. Subsequent blocking of one or both electrophilic axes on the iodine-based Lewis acids also led to markedly reduced binding constants, even when potentially suitable substrates were used, further corroborating our findings. This trend could also be identified by supporting DFT calculations, but these tend to (sometimes severely) underestimate the binding constants, even when intrinsic solvation models were applied. A crystal structure between a diamide and the unhindered iodolium compound also clearly demonstrated biaxial binding. This study constitutes an important first step toward the rational exploitation of the two electrophilic axes in iodine(III)-based Lewis acids, and experiments to utilize this concept in organocatalysis are currently underway.[33]

ASSOCIATED CONTENT

Supporting Information

The Supporting Information is available free of charge at https://pubs.acs.org/doi/10.1021/jacs.9b13309.

Full experimental details, characterization data, ITC spectra (PDF)
X-ray structural analysis (CIF, CIF)
Input and output files of DFT calculations (CIF)
Coordinates and energies of DFT calculations (CIF)

AUTHOR INFORMATION

Corresponding Author

Stefan M. Huber − *Fakultät für Chemie und Biochemie, Organische Chemie I, Ruhr-Universität Bochum, 44801 Bochum, Germany;* orcid.org/0000-0002-4125-159X; Email: stefan.m.huber@rub.de

Authors

Flemming Heinen − *Fakultät für Chemie und Biochemie, Organische Chemie I, Ruhr-Universität Bochum, 44801 Bochum, Germany*

Elric Engelage − *Fakultät für Chemie und Biochemie, Organische Chemie I, Ruhr-Universität Bochum, 44801 Bochum, Germany*

Christopher J. Cramer − *Department of Chemistry, Chemical Theory Center, and Minnesota Supercomputing Institute, University of Minnesota, Minneapolis 55455-0431, Minnesota, United States;* orcid.org/0000-0001-5048-1859

Complete contact information is available at: https://pubs.acs.org/10.1021/jacs.9b13309

Notes

The authors declare no competing financial interest.

ACKNOWLEDGMENTS

This project received funding from the European Research Council under the European Union's Horizon 2020 research and innovation programme (638337). Funded by the Deutsche Forschungsgemeinschaft (German Research Foundation) under Germany's Excellence Strategy-EXC 2033-390677874-RESOLV.

REFERENCES

(1) (a) Yoshimura, A.; Zhdankin, V. V. Advances in Synthetic Applications of Hypervalent Iodine Compounds. *Chem. Rev.* **2016**, *116*, 3328−3435. (b) Kumar, R.; Wirth, T. Asymmetric Synthesis with Hypervalent Iodine Reagentsa. *Top. Curr. Chem.* **2015**, *373*, 243−261. (c) Silva, L. F., Jr.; Olofsson, B. Hypervalent iodine reagents in the total synthesis of natural products. *Nat. Prod. Rep.* **2011**, *28*, 1722−1754.

(2) (a) Vita, M. V.; Waser, J. Cyclic Hypervalent Iodine Reagents and Iron Catalysts: The Winning Team for Late-Stage C-H Azidation. *Angew. Chem., Int. Ed.* **2015**, *54*, 5290−5292. (b) Brunner, C.; Andries-Ulmer, A.; Kiefl, G. M.; Gulder, T. Hypervalent Fluoroiodane-Triggered Synthesis of Fluoro-Azabenzoxazepines and Azaindoles. *Eur. J. Org. Chem.* **2018**, *2018*, 2615−2621. (c)) Uyanik, M.; Yasui, T.; Ishihara, K. Chiral Hypervalent Organoiodine-Catalyzed Enantioselective Oxidative Spirolactonization of Napthol Derivatives. *J. Org. Chem.* **2017**, *82*, 11946−11953.

(3) (a) Olofsson, B. Arylation with Diaryliodonium salts. In *Hypervalent Iodine Chemistry;* Wirth, T., Ed.; Topics in Current Chemistry, Springer International Publishing, 2016; Vol. *373*, pp 135−165. (b) Boelke, A.; Finkbeiner, P.; Nachtsheim, B. J. Atom-economical group-transfer reactions with hypervalent iodine compounds. *Beilstein J. Org. Chem.* **2018**, *14*, 1263−1280. (c) Zhu, D.; Wu, Y.; Wu, B.; Luo, B.; Ganesan, A.; Wu, F.-H.; Pi, R.; Huang, P.; Wen, S. Three-component Pd/Cu-catalyzed cascade reactions of cyclic iodoniums, alkynes, and boronic acids: an approach to methylidenefluorenes. *Org. Lett.* **2014**, *16*, 2350−2353.

(4) (a) Robidas, R.; Guérin, V.; Provençal, L.; Echeverria, M.; Legault, C. Y. Investigations of Iodonium Trifluoroborate Zwitterions as

Bifunctional Arene Reagents. *Org. Lett.* **2017**, *19*, 6420−6423. (b)) Kita, Y.; Morimoto, K.; Ito, M.; Ogawa, C.; Goto, A.; Dohi, T. Metal-Free Oxidative Cross-Coupling of Unfunctionalized Aromatic Compounds. *J. Am. Chem. Soc.* **2009**, *131*, 1668−1669.

(5) (a) Cavallo, G.; Metrangolo, P.; Milani, R.; Pilati, T.; Priimagi, A.; Resnati, G.; Terraneo, G. The Halogen Bond. *Chem. Rev.* **2016**, *116*, 2478−2601. (b) Brown, A.; Beer, P. D. Halogen bonding anion recognition. *Chem. Commun.* **2016**, *52*, 8645−8658.

(6) (a) Politzer, P.; Lane, P.; Concha, M.; Ma, Y.; Murray, J. An overview of halogen bonding. *J. Mol. Model.* **2007**, *13*, 305−311. (b) Politzer, P.; Murray, J. S.; Concha, M. C. Halogen bonding and the design of new materials: organic bromides, chlorides and perhaps even fluorides as donors. *J. Mol. Model.* **2007**, *13*, 643−650.

(7) (a) Bent, H. A. Structural chemistry of donor-acceptor interactions. *Chem. Rev.* **1968**, *68*, 587−648. (b) Reed, A. E.; Weinhold, F.; Weiss, R.; Macheleid, J. Nature of the contact ion pair trichloromethyl-chloride (CCl3+Cl-). A theoretical study. *J. Phys. Chem.* **1985**, *89*, 2688−2694.

(8) (a) Mukherjee, A.; Tothadi, S.; Desiraju, G. R. Halogen Bonds in Crystal Engineering: Like Hydrogen Bonds yet Different. *Acc. Chem. Res.* **2014**, *47*, 2514−2524. (b) Nikolayenko, V. I.; Castell, D. C.; van Heerden, D. P.; Barbour, L. J. Guest-Induced Structural Transformations in a Porous Halogen-Bonded Framework. *Angew. Chem., Int. Ed.* **2018**, *57*, 12086−12091.

(9) (a) Yan, X.; Zou, K.; Cao, J.; Li, X.; Zhao, Z.; Li, Z.; Wu, A.; Liang, W.; Mo, Y.; Jiang, Y. Single-handed supramolecular double helix of homochiral bis(N-amidothiourea) supported by double crossed C-I•••S halogen bonds. *Nat. Commun.* **2019**, *10*, 3610. (b) Bunchuay, T.; Docker, A.; Martinez-Martinez, A. J.; Beer, P. D. A Potent Halogen-Bonding Donor Motif for Anion Recognition and Anion Template Mechanical Bond Synthesis. *Angew. Chem., Int. Ed.* **2019**, *58*, 13823−13827.

(10) (a) Sutar, R. L.; Huber, S. M. Catalysis of Organic Reactions through Halogen Bonding. *ACS Catal.* **2019**, *9*, 9622−9639. (b) Bamberger, J.; Ostler, F.; Mancheño, O. G. Frontiers in Halogen and Chalcogen-Bond Donor Organocatalysis. *ChemCatChem* **2019**, *11*, 5198−5211.

(11) Zhang, Y.; Han, J.; Liu, Z.-J. Diaryliodonium salts as efficient Lewis acid catalyst for direct three component Mannich reactions. *RSC Adv.* **2015**, *5*, 25485−25488.

(12) (a) Labattut, A.; Tremblay, P.-L.; Moutounet, O.; Legault, C. Y. Experimental and Theoretical Quantification of the Lewis Acidity of Iodine(III) Species. *J. Org. Chem.* **2017**, *82*, 11891−11896. (b) Mayer, R. J.; Ofial, A. R.; Mayr, H.; Legault, C. L. Lewis Acidity Scale of Diaryliodonium Ions toward Oxygen, Nitrogen, and Halogen Lewis Bases. *J. Am. Chem. Soc.* **2020**, *142*, 5221−5233.

(13) Heinen, F.; Engelage, E.; Dreger, A.; Weiss, R.; Huber, S. M. Iodine(III) Derivatives as Halogen Bonding Organocatalysts. *Angew. Chem., Int. Ed.* **2018**, *57*, 3830−3833.

(14) (a) Kirshenboim, O.; Kozuch, S. How to Twist, Split and Warp a σ-hole with Hypervalent Halogens. *J. Phys. Chem. A* **2016**, *120*, 9431−9445. (b) Catalano, L.; Cavallo, G.; Metrangolo, P.; Resnati, G. Halogen Bonding in Hypervalent Iodine Compounds. In *Hypervalent Iodine Chemistry;* Wirth, T., Ed.; Topics in Current Chemistry, Springer: Cham, Switzerland, 2016; Vol. 373, pp 289−309.

(15) (a) Alcock, N. W.; Countryman, R. M. Secondary bonding. Part 1. Crystal and molecular structures of $(C_6H_5)_2IX$ (X = Cl, Br, or I). *J. Chem. Soc., Dalton Trans.* **1977**, *3*, 217−219. (b) Cavallo, G.; Murray, J. S.; Politzer, P.; Pilati, T.; Ursini, M.; Resnati, G. Halogen bonding in hypervalent iodine and bromine derivatives: halonium salts. *IUCrJ* **2017**, *4*, 411−419.

(16) (a) Ochiai, M.; Suefuji, T.; Miyamoto, K.; Tada, N.; Goto, S.; Shiro, M.; Sakamoto, S.; Yamaguchi, K. Secondary hypervalent I(III):::O interactions: synthesis and structure of hypervalent complexes of diphenyl- λ^3-iodanes with 18-crown-6. *J. Am. Chem. Soc.* **2003**, *125*, 769−773. (b) Ochiai, M.; Miyamoto, K.; Suefuji, T.; Sakamoto, S.; Yamaguchi, K.; Shiro, M. Synthesis, Characterization, and Reaction of Ethynyl(phenyl)-λ^3-Iodane Complex with [18]Crown-6. *Angew. Chem., Int. Ed.* **2003**, *42*, 2191−2194. (c) Ochiai, M.; Miyamoto, K.; Suefuji, T.; Shiro, M.; Sakamoto, S.; Yamaguchi, K. Synthesis and structure of supramolecular complexes between 1-alkynyl(phenyl)(tetrafluoroborato)-λ^3-iodanes and 18-crown-6. *Tetrahedron* **2003**, *59*, 10153−10158. (d) Miyamoto, K.; Hirobe, M.; Saito, M.; Shiro, M.; Ochiai, M. One-Pot Regioselective Synthesis of Chromanyl(phenyl)-λ^3-iodanes: Tandem Oxidative Cylization and λ^3-Iodanation of 3-Phenylpropanols. *Org. Lett.* **2007**, *9* (10), 1995−1998.

(17) Zhao, Y.; Truhlar, D. G. The M06 suite of density functionals for main group thermochemistry, thermochemical kinetics, noncovalent interactions, excited states, and transitions elements: two new functionals and systematic testing of four M06-class functionals and 12 other functionals. *Theor. Chem. Acc.* **2008**, *120*, 215−241.

(18) (a) Weigend, F.; Ahlrichs, R. Balanced basis sets of split valence, triple zeta valence and quardruple zeta valence quality for H to Rn: Design and assessment of accuracy. *Phys. Chem. Chem. Phys.* **2005**, *7*, 3297−3305. (b) Rappoport, D.; Furche, F. *J. Chem. Phys.* **2010**, *133*, 134105.

(19) (a) Marenich, A. V.; Cramer, C. J.; Truhlar, D. G. Universal Solvation Model Based on Solute Electron Density and on a Continuum Model of the Solvent Defined by the Bulk Dielectric Constant and Atomic Surface Tensions. *J. Phys. Chem. B* **2009**, *113*, 6378−6396. (b) Engelage, E.; Schulz, N.; Heinen, F.; Huber, S. M.; Truhlar, D. G.; Cramer, C. J. Refined SMD Parameters for Bromine and Iodine Accurately Model Halogen-Bonding Interactions in Solution. *Chem. - Eur. J.* **2018**, *24*, 15983−15987.

(20) CYLview, 1.0b; C. Y. Legault, Université de Sherbrooke 2009 (http://www.cylview.org).

(21) Bondi, A. van der Waals Volumes and Radii. *J. Phys. Chem.* **1964**, *68*, 441−451.

(22) Frisch, M. J.; Trucks, G. W.; Schlegel, H. B.; Scuseria, G. E.; Robb, M. A.; Cheeseman, J. R.; Scalmani, G.; Barone, V.; Petersson, G. A.; Nakatsuji, H.; Li, X.; Caricato, M.; Marenich, A. V.; Bloino, J.; Janesko, B. G.; Gomperts, R.; Mennucci, B.; Hratchian, H. P.; Ortiz, J. V.; Izmaylov, A. F.; Sonnenberg, J. L.; Williams-Young, D., Ding, F.; Lipparini, F.; Egidi, F.; Goings, J.; Peng, B.; Petrone, A.; Henderson, T.; Ranasinghe, D.; Zakrzewski, V. G.; Gao, J.; Rega, N.; Zheng, G.; Liang, W.; Hada, M.; Ehara, M.; Toyota, K.; Fukuda, R.; Hasegawa, J.; Ishida, M.; Nakajima, T.; Honda, Y.; Kitao, O.; Nakai, H.; Vreven, T.; Throssell, K.; Montgomery, J. A., Jr.; Peralta, J. E.; Ogliaro, F.; Bearpark, M. J.; Heyd, J. J.; Brothers, E. N.; Kudin, K. N.; Staroverov, V. N.; Keith, T. A.; Kobayashi, R.; Normand, J.; Raghavachari, K.; Rendell, A. P.; Burant, J. C.; Iyengar, S. S.; Tomasi, J.; Cossi, M.; Millam, J. M.; Klene, M.; Adamo, C.; Cammi, R.; Ochterski, J. W.; Martin, R. L.; Morokuma, K.; Farkas, O.; Foresman, J. B.; Fox, D. J. *Gaussian 16,* Rev. B.01; Gaussian, Inc.: Wallingford, CT, 2016.

(23) See also: Engelage, E.; Reinhard, D.; Huber, S. M. Is there a Single Ideal Parameter for Halogen-Bonding-Based Lewis Acidity? *Chem. - Eur. J.* **2020**, *26*, 3843−3861.

(24) To this end, the radius of iodine was set to 2.74 Å using the modifysph command; see ref 19 for a sample input file.

(25) Grimme, S. Supramolecular Binding Thermodynamics by Dispersion-Corrected Density Functional Theory. *Chem. - Eur. J.* **2012**, *18*, 9955−9964.

(26) (a) Scalmani, G.; Frisch, M. J. Continuous surface charge polarizable continuum models of solvation. I. General for-malism. *J. Chem. Phys.* **2010**, *132*, 114110. (b) Tomasi, J.; Mennucci, B.; Cammi, R. Quantum mechanical continuum solvation models. *Chem. Rev.* **2005**, *105*, 2999−3093.

(27) (a) Reed, A. E.; Weinstock, R. B.; Weinhold, F. Natural population analysis. *J. Chem. Phys.* **1985**, *83*, 735−746. (b) Reed, A. E.; Curtiss, L. A.; Weinhold, F. Intermolecular interactions from a natural bond orbital, donor-acceptor viewpoint. *Chem. Rev.* **1988**, *88*, 899−926.

(28) Mulliken, R. S. Molecular Compounds and their Spectra. III. The Interaction of Electron Donors and Acceptors. *J. Phys. Chem.* **1952**, *56* (7), 801−822.

(29) Bader, R. F. W. A quantum theory of molecular structure and its applications. *Chem. Rev.* **1991**, *91*, 893−928.

https://dx.doi.org/10.1021/jacs.9b13309
J. Am. Chem. Soc. 2020, 142, 8633−8640

(30) Lu, T.; Chen, F. Multiwfn: a multifunctional wavefunction analyzer. *J. Comput. Chem.* **2012**, *33*, 580−592.
(31) Kumar, P. S. V.; Raghavendra, V.; Subramanian, V. Bader's Theory of Atoms in Molecules (AIM) and its Applications to Chemical Bonding. *J. Chem. Sci.* **2016**, *128*, 1527−1536.
(32) Johnson, E. R.; Keinan, S.; Mori-Sánchez, P.; Contreras-García, J.; Cohen, A. J.; Yang, W. Revealing noncovalent interactions. *J. Am. Chem. Soc.* **2010**, *132*, 6498−6506.
(33) Iodolium compounds like **4a**/**Cl**, also known as diphenyleneiodonium chloride (DPIC), possess biological activity, e.g., as NADH/NADPH oxidase inhibitors (Bloxham, D. P. The Relationship of Diphenyleneiodonium-Induced Hypoglycaemia to the Specific Covalent Modification of NADH-Ubiquinone Oxidoreductase, *Biochem. Soc. Trans.* **1979**, *7*, 103−106), as antibiotics (Pandey, M.; Singh, A. K.; Thakare, R.; Talwar, S.; Karaulia, P.; Dasgupta, A.; Chopra, S.; Pandey, A. K. Diphenyleneiodonium chloride (DPIC) displays broad-spectrum bactericidal activity, *Sci. Rep.* **2017**, *7*: 11521), and as hypoglycemic agents (Holland, P. C.; Clark, M. G.; Bloxham, D. P.; Lardy, H. A. Mechanism of action of the hypoglycemicagent diphenyleneiodonium, *J. Biol. Chem.* **1973**, *248*, 6050−6056.). Thus, our findings may help to furtherelucidate the binding mode of these compounds to their target proteins.

https://dx.doi.org/10.1021/jacs.9b13309
J. Am. Chem. Soc. 2020, 142, 8633−8640